

BBA 33036

## Spectroscopic properties of the hydroxylase of methane monooxygenase

Roger C. Prince, Graham N. George, Judith C. Savas, Stephen P. Cramer \*  
and Ramesh N. Patel \*\*

*Exxon Research and Engineering Co., Annandale, NJ (U.S.A.)*

(Received 27 July 1987)

Key words: Methane monooxygenase; Hydroxylase; Spectroscopic property; ESR; X-ray spectroscopy

The hydroxylase component of methane monooxygenase (EC 1.14.13.25), which catalyzes the oxidation of methane to methanol, has been studied by visible, electron spin resonance and X-ray spectroscopies. The enzyme appears to possess a  $\mu$ -oxo- or  $\mu$ -hydroxo-bridged binuclear iron site, with no sulfur ligands to the cluster. Each Fe has 4–6 oxygen (or nitrogen) ligands, at an average distance of  $1.92 \pm 0.03$  Å. The Fe-Fe distance is  $3.05 \pm 0.05$  Å. Essentially all of the irons are in the  $\text{Fe}^{3+}$  state as the enzyme is prepared, but reduction with *N*-methylphenazonium methosulfate generates ESR-detectable states that appear to emanate from mixed-valence binuclear sites. One of these, with  $g_{av}$  near 1.85, displays typical Curie law microwave saturation behavior, but the other, with  $g_{av}$  near 1.73, has a very potent method of spin-relaxation. Together they account for approximately 0.6 spins per molecule.

### Introduction

The diverse group of organisms capable of living on methane as the sole source of carbon and energy were first described at the beginning of the century. Nevertheless, it has only been in the last decade or so that their physiology, ecology and biochemistry have received much attention (see Refs. 1 and 2). Methanotrophic bacteria can be divided into two classes, I and II, dependent on the structure of their internal membranes and on the pathways of assimilation of one carbon units; Type I organisms use the ribulose monophosphate

pathway for the assimilation of carbon at the level of formaldehyde, and have bundles of internal membranes throughout the cell that appear to be invaginations of the cytoplasmic membrane. Type II organisms assimilate formaldehyde by the serine pathway, and have paired peripheral membranes within the cell [1]. Both types of organisms metabolize methane by first hydroxylating it to methanol, using the enzyme methane monooxygenase (EC 1.14.13.25). Under some conditions this activity is found in soluble extracts of cells; under others, the activity appears to be associated with the membrane. There is some confusion over what regulates the apparently different activities, but high copper concentrations or low oxygen tension favor the membrane-bound enzyme [3,4].

Both soluble [5,6] and membrane-bound [7] forms of the enzyme system have been isolated, but the former has been rather more characterized. Dalton and his colleagues have isolated a three-component system from *Methylococcus capsulatus* (Bath) composed of a hydroxylase

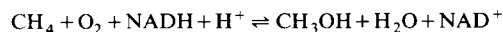
\* Present address: Schlumberger-Doll Research, Ridgefield CT 06877–4108, U.S.A.

\*\* Present address: E.R. Squibb and Sons, P.O. Box 191, New Brunswick, NJ 08903, U.S.A.

Correspondence: R.C. Prince, Exxon Research and Engineering Co., Clinton Township, Route 22 East, Annandale, NJ 08801, U.S.A.

(Component A), a colorless protein (Component B), and a flavoprotein (Component C) [5,8]. Patel and his colleagues have isolated a two component system from *Methylobacterium* CRL-26 [6,9], which seems to lack the Component B of the Dalton preparation.

All these soluble preparations catalyze the reaction



The actual oxidation of methane is thought to occur on the hydroxylase (Component A), while the oxidation of NADH occurs on the flavoprotein. Component B, in the system where it is known to be present, appears to regulate the interaction of these two proteins [5–9].

The flavoprotein has been extensively studied [10,11]. It contains an  $\text{Fe}_2\text{S}_2$  center with  $E_{m,7} - 247$  mV, and FAD with  $E_{m,7} - 195$  and  $-250$  mV for the FAD/FAD · H and FAD · H/FADH<sub>2</sub> couples.

The hydroxylase has not been as well characterized, although Woodland et al. [8] have recently presented both ESR and thermodynamic data on its metal center. They interpreted their results as indicative of a binuclear Fe center, perhaps of the hemerythrin type. In this paper we present further ESR data on this center, together with the first X-ray spectroscopic data. Our results confirm and extend the data of Woodland et al., and extend them to both types of methanotrophic bacteria. The soluble hydroxylase component of methane monooxygenase joins hemerythrin [12], ribonucleotide reductase [13], purple acid phosphatase [14] and uteroferrin [14] in a group of proteins with  $\mu$ -oxo- or  $\mu$ -hydroxo-linked binuclear Fe sites as the prosthetic group.

## Materials and Methods

*Methylococcus* CRL-25, a Type I methanotroph, and *Methylobacterium* CRL-26, a Type II organism, were grown with methane as the sole source of carbon and energy as previously described [6,9,15]. The hydroxylase component was purified anaerobically, using DEAE-cellulose, QAE-Sephadex and Bio-Gel-Agarose chromatography, while the flavoprotein was purified by

DEAE-cellulose chromatography [6,9,15]. Enzyme activity was determined by the epoxidation of propylene [6,9,15]; the specific activity of samples used in this work was between 150 and 200 nmol propylene epoxidized/mg hydroxylase per min [15]. Metal analysis revealed  $2.8 \pm 0.2$  Fe and  $0.5 \pm 0.1$  Zn per  $\alpha_2\beta_2\gamma_2$  hydroxylase [15].

Optical spectra were taken with a Perkin-Elmer 559A spectrometer, while electron spin resonance spectra were obtained with a Varian E-109 spectrometer, equipped with an Oxford flowing helium cryostat and EIP model 548A microwave frequency counter. Temperatures were calibrated from the amplitude of the ESR signal of a Cu-ethylenediamine tetraacetate standard under non-saturating microwave powers. This standard was also used as the standard for spin integrations, which were performed taking into account the necessary corrections for transition probability according to Aasa and Vanngard [16]. X-ray absorption spectra were recorded at the Stanford Synchrotron Radiation Laboratory, using a Si[2,2,0] monochromator on line VII-3 with fluorescence detection [17,18]. The samples were maintained at a temperature near 4 K in an Oxford Instruments cryostat during data collection.

EXAFS data were analyzed quantitatively by curve fitting to the following approximate expression:

$$\chi(k) \cong \sum_b \frac{N_b S_b A_b(k)}{k R_{ab}^2} e^{-2\sigma_{ab}^2 k^2} \sin[2k R_{ab} + \phi_{ab}(k)]$$

Where  $k$  is the photoelectron wave number,  $N_b$  is the number of  $b$  type atoms at a mean distance  $R_{ab}$  from the absorber  $a$ .  $\sigma_{ab}$  is the root mean square deviation in  $R_{ab}$  (the Debye-Waller factor).  $A(k)$  and  $\phi(k)$  are the amplitude and phase functions, respectively, and were those tabulated by Teo and Lee [19], with scalar corrections,  $S_b$ , to the amplitude function determined from appropriate models; *Clostridium pasteurianum* ferredoxin, and Fe(acetylacetonate)<sub>3</sub>.

## Results

Fig. 1 shows the optical absorption spectra of the hydroxylase components of the two organisms studied in this work. There is a pronounced spec-

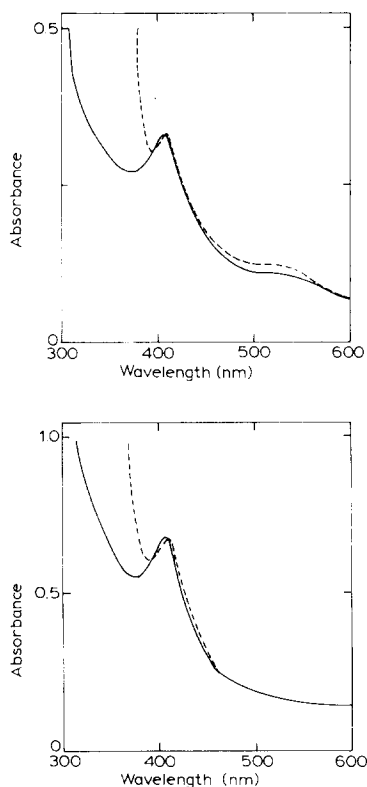


Fig. 1. Optical absorption spectra of methan monooxygenase. Enzyme from *Methylobacterium* CRL-26 (top, at 15 mg/ml) and *Methylococcus* CRL-25 (bottom, at 12 mg/ml) in 50 mM potassium phosphate (pH 7.0). The broken lines represent spectra of dithionite-reduced samples.

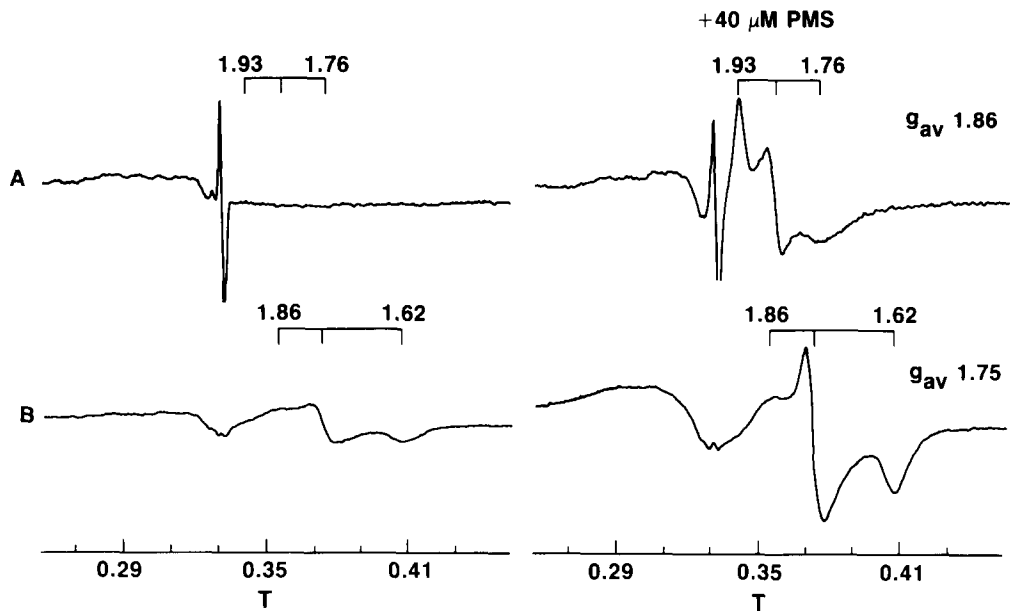
tral feature at 408 nm in both preparations. The spectra are rather similar to those described for the hydroxylase of *M. capsulatus* (Bath) in Table III of Ref. 20, although the feature at 408 nm was only seen as a shoulder in their preparations, and this was not always present.

Figs. 2 and 3 show the ESR spectra of the two preparations. Two distinct ESR spectra are displayed by both enzymes. One, best seen at temperatures near 17 K with 10 mW of applied microwave power, has an apparent  $g_{av}$  near  $g = 1.85$ . This is similar to the spectrum recorded under similar conditions by Woodland et al. [8]. The second is best seen at colder temperatures and with rather more power; 6 K and 100 mW of applied microwave power gave good spectra on our spectrometer. This signal is broader than the

one seen at warmer temperatures, with an apparent  $g_{av}$  near  $g = 1.74$ . Both signals have 'rhombic' lineshapes, and display considerable linewidth anisotropy. It is noteworthy that neither signal was prominent in any of our preparations unless *N*-methylphenazonium methosulfate was added (Figs. 2 and 3). This compound was initially added as a mediator for a redox titration; it has  $E_{m,7}$  near 85 mV [21], and is a potent mediator of electrons between redox centers in proteins and metal electrodes. Despite many attempts with a range of redox mediators (see Ref. 21), and in the presence or absence of the flavoprotein, our redox titrations did not yield reproducible Nernstian behavior (see, for example, Ref. 8). Nevertheless, we invariably saw the behavior shown in Figs. 2 and 3; the protein initially showed only small amounts of the lower temperature signal, but upon addition of the redox mediator, and with subsequent incubation, both ESR signals grew in. With 40  $\mu$ M *N*-methylphenazonium methosulfate the signals had attained maximal size after 30 minutes at room temperature. The fact that the low temperature signal was present without the redox dye, while the higher temperature signal was absent, indicates that the two different ESR signals are not in ready equilibrium with each other. Enzyme activity assays of the hydroxylases showed equal activity in the presence or absence of the *N*-methylphenazonium methosulfate, but unfortunately the conditions of the activity assay [6,9,15] require dilute samples, and measurable activity is very low at the high concentrations required for ESR spectroscopy, so we are unable to draw any firm conclusions about whether both, either, or neither of the ESR signals is associated with enzyme turnover.

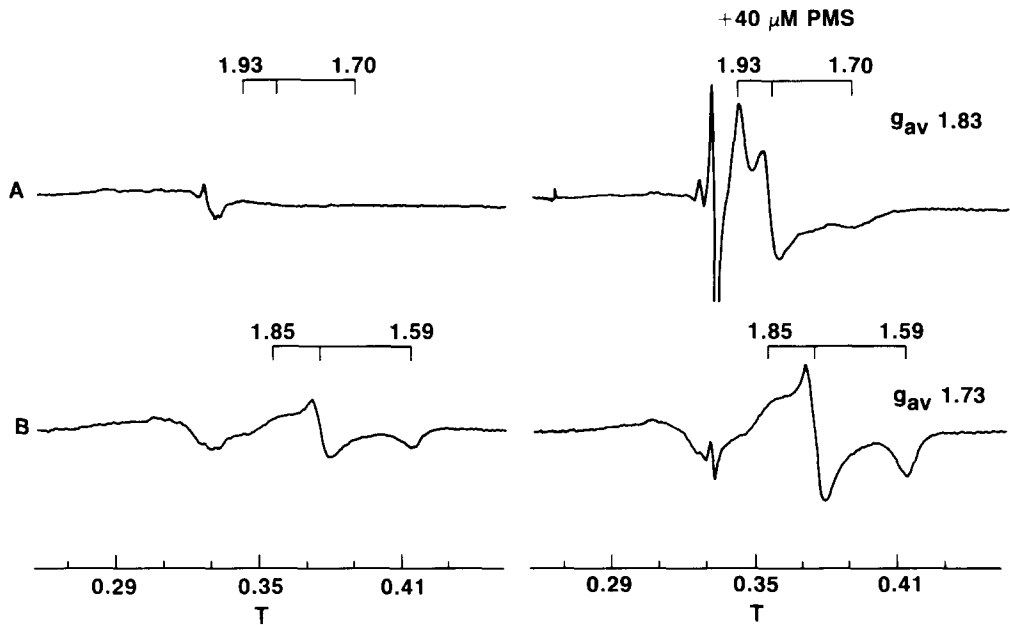
While the proteins from the two organisms show very similar ESR spectra, small differences are seen. For example, the  $g_{av}$  1.85 signal from *Methylococcus* CRL-25 appears to be a mixture of a signal with  $g_x$  1.70 and another with  $g_x$  1.78. Computer simulations (not illustrated) indicate that the latter is about 20% of the total signal intensity. In contrast, the  $g_{av}$  1.85 signal of *Methylobacterium* CRL-26 seems spectrally 'pure'.

As can be seen in Figs. 2 and 3, some preparations had narrow ESR signals at  $g = 2$  in the absence of added redox mediators. Similarly, some



RP595

Fig. 2. Electron spin resonance spectra of methane monooxygenase from *Methylobacterium* CRL-26. Enzyme (11 mg/ml) in 50 mM potassium phosphate (pH 7.0). The samples on the right was supplemented with 40  $\mu$ M *N*-methylphenazonium methosulfate and incubated for 15 min prior to freezing. Spectra on top row (A) were recorded at 16 K with 20 mW of applied power and 1.6 mT modulation. Spectra on the bottom (B) were recorded at 6 K with 100 mW of applied power and 1.6 mT modulation.



RP596

Fig. 3. Electron spin resonance spectra of methane monooxygenase from *Methylococcus* CRL-25. Enzyme (16 mg/ml) was dissolved in the buffer used in Fig. 2, and measured as in Fig. 2.

preparations had signals near  $g = 4.3$ . Neither of these signals appeared in all samples, and we believe their presence in some samples to be due to adventitious contamination.

The microwave saturation behavior of the ESR signals from the two preparations were very similar. At low temperature the  $g_{av}$  1.85 signal saturates readily ( $P_{1/2} = 0.44$  mW), and follows a Curie Law temperature dependence (Fig. 4A), but the  $g_{av}$  1.74 signal could not be saturated even at the highest powers ( $P_2 > 500$  mW) (Fig. 4B). No

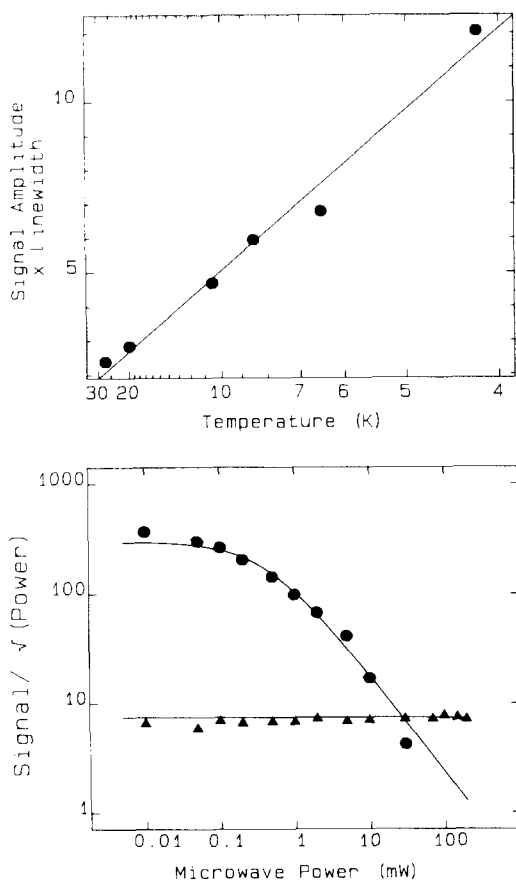


Fig. 4. Temperature dependence (A) and microwave saturation behavior (B) of the ESR signals of methane monooxygenase. The samples used in Figs. 2 (for A) and 3 (for B) were used. (A) shows the Curie Law behavior of the  $g_{av}$  1.86 signal of the enzyme from *Methylobacterium* CRL-26. (B) shows the microwave power saturation profiles of the  $g_{av}$  1.83 (●) and  $g_{av}$  1.73 (▲) signals of the enzyme from *Methylococcus* CRL-25. The data were fit to the equation of Beinert and Orme-Johnson [38].

TABLE I

SPIN QUANTITATION OF THE ESR SPECTRA OF THE HYDROXYLASES

The  $g_{av}$  1.85 signal was measured at 10 K with 10 mW of applied microwave power, the  $g_{av}$  1.74 signal at 6 K with 100 mW of applied microwave power.

	$g_{av}$ 1.85	$g_{av}$ 1.74	Total
<i>Methylococcus</i> CRL-25	0.49	0.12	0.61
<i>Methylobacterium</i> CRL-26	0.24	0.29	0.53

marked anisotropy was observed in the saturation of the  $g_{av}$  1.85 signal. The saturation properties of both ESR signals of both organisms were essentially indistinguishable.

Spin quantitation of the ESR signals yielded the data of Table I. The value for the  $g_{av}$  1.85 center may be compared with the value of 0.27 spins per protein determined for the hydroxylase from *M. capsulatus* (Bath) by Woodland et al. [8]. Another, less well defined, broad ESR signal (Figs. 2 and 3) centered near  $g = 2.05$  is also seen in both preparations. This signal, like the  $g_{av}$  1.74 signal, was resistant to microwave power saturation. The  $g$  2.05 signal could not be accurately integrated because of its apparently large linewidth, but it seems probable that it contributes significantly to the total number of spins.

The iron X-ray absorption edge of the hydroxylase from *Methylobacterium* CRL-26 is illustrated in Fig. 5. A weak but distinct pre-edge

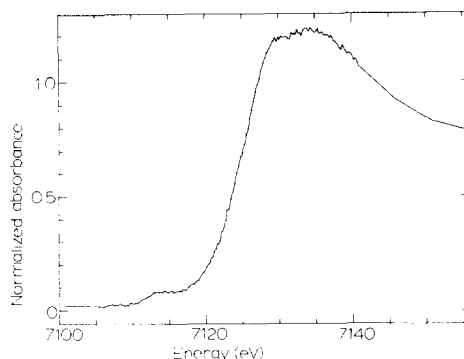


Fig. 5. Iron K-edge XANES spectrum of methane monooxygenase of *Methylobacterium* CRL-26. The spectrum was recorded at a temperature close to 4.2 K.

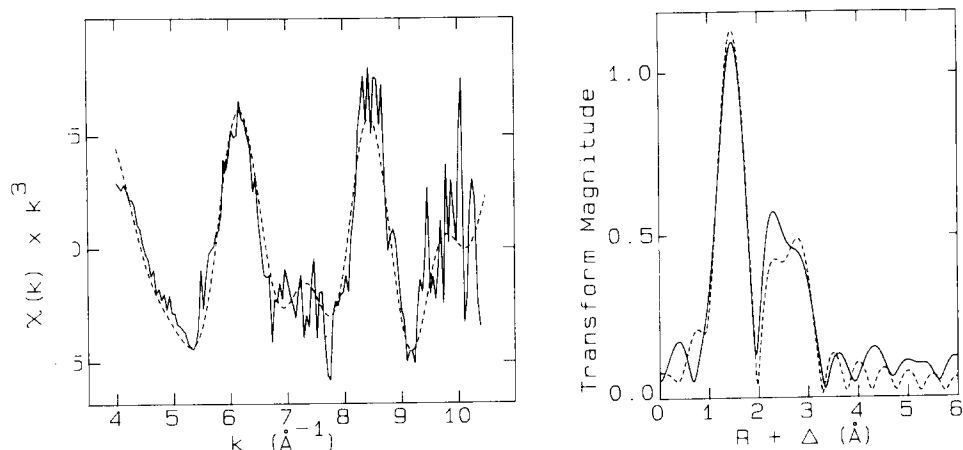


Fig. 6. Iron EXAFS and Fourier transform of methane monooxygenase from *Methylobacterium* CRL-26. The solid lines are the data, and the dashed lines are the best fit summarized in Table II.

feature attributable to the  $1s \rightarrow 3d$  bound state transition is present at about 7113 eV. Although the  $1s \rightarrow 3d$  transitions are dipole-forbidden, they can gain intensity by mixing with  $p$  levels. Thus the feature is more intense in species with tetrahedrally coordinated iron, such as iron-sulfur clusters [22]. In the hydroxylase spectrum (Fig. 5) the  $1s \rightarrow 3d$  transition is not present as a well defined peak, but rather as a shoulder. The small size of the feature precludes a tetrahedrally coordinated iron site. A comparison of the edge position with that of model compounds (23) indicates that the edge position is characteristic of ferric iron. Furthermore, such comparisons show little similarities to compounds with iron-sulfur coordination.

TABLE II  
EXAFS CURVE FITTING RESULTS

Interaction	$N$	$R$ (Å)	$\sigma^2$ (Å <sup>2</sup> )	Error <sup>a</sup>
Fe-O	4	1.922	0.0018	1.028 <sup>b</sup>
	5	1.922	0.0038	1.284 <sup>b</sup>
	6	1.923	0.0056	1.631 <sup>b</sup>
Fe-Fe	1.7	3.049	0.0025	<sup>c</sup>

<sup>a</sup> Fit error was defined as  $\{\sum(\chi_{\text{obs}} - \chi_{\text{calc}})^2 k^6\}/n$  where  $n$  is the number of data points,  $\chi_{\text{obs}}$  the experimental EXAFS, and  $\chi_{\text{calc}}$  the calculated EXAFS. The summation is over all ( $n$ ) data points.

<sup>b</sup>  $N$  was fixed,  $R$  and  $\sigma$  varied.

<sup>c</sup> All parameters were varied.

The iron extended X-ray absorption fine structure (EXAFS) Fourier transform is shown in Fig. 6. The Fourier transform clearly indicates the presence of strong interactions with at least two shells of neighboring atoms. The major peak in the transform at  $R + \Delta = 1.4$  Å is attributable to Fe-(O or N) interactions, while the smaller peak at  $R + \Delta = 2.5$  Å is attributable to more distant Fe-Fe interactions.

EXAFS is not good at discriminating individual components from mixtures of species, and when a mixture is present, as is probable in the present case, analysis of EXAFS spectra yields an average set of distances and coordination numbers for the entire population. Nevertheless, such averages can be very informative. The two shell fit to the EXAFS data is illustrated in Fig. 6, and summarized in Table II. There are between 4 and 6 Fe-O,N interactions with a mean bond length of 1.92 Å, and 1-2 Fe-Fe interactions with an Fe-Fe distance of 3.05 Å. As is usual in EXAFS analysis, the fits do not distinguish between scatterers of similar atomic number, such as oxygen and nitrogen.

## Discussion

Taken together, the data presented in this paper provide strong evidence that the metal center of the hydroxylase of the soluble methane monooxygenase is a binuclear iron cluster with oxygen

and/or nitrogen ligands. Such a structure would be similar to that reported in hemerythrin [12], ribonucleotide reductase [13], purple acid phosphatase [14] and uteroferrin [14]. All apparently possess a  $\mu$ -oxo- or a  $\mu$ -hydroxo-linked binuclear Fe site as the prosthetic group, but there are significant differences between the different proteins.

Hemerythrin is the oxygen transport protein in the coelomic fluid of sipunculid (and a few apparently unrelated) marine worms. While it is functionally analogous to hemoglobin, its mechanism of oxygen binding is quite distinct, for while the deoxygenated form contains two ferrous iron atoms, the oxygenated form is best described as possessing two ferric atoms. Such reversible oxidation of the iron upon oxygenation does not occur in hemoglobin [12]. An additional form, methemerythrin, contains two ferric atoms in the absence of oxygen. This form will not bind oxygen, and its physiological role is obscure. The visible absorption spectra of hemerythrin are much less intense than those of hemoglobin, and deoxyhemerythrin has no bands above 300 nm [24]. Oxyhemerythrin has intense bands near 330 and 360 nm, and broader ones near 500 and 700 nm, but none near 408 nm. Neither deoxy-, oxy- or met-hemerythrin display ESR spectra, but the mixed valence 'semi-met'-hemerythrin, possessing one ferrous and one ferric iron, does. Indeed this species displays different spectra depending on whether it was obtained by the one electron reduction of methemerythrin, (semi-met)<sub>R</sub>, or the one electron oxidation of deoxyhemerythrin, (semi-met)<sub>O</sub>. The former is rather axial, with  $g_{av}$  near 1.79, while the latter is more rhombic, with  $g_{av}$  near 1.83 (Fig. 5 in Ref. 12). Both are seen under conditions appropriate for the  $g_{av}$  1.83 signals of the methane monooxygenase hydroxylase (Figs. 2 and 3); no evidence for a broader signal at lower temperature, analogous to the  $g_{av}$  1.74 signal of the hydroxylase, was seen by Muhoberac et al. [25]. The X-ray absorption spectra of deoxy-, oxy-, metazido- and methydroxo-hemerythrin have been examined by Stern and co-workers [26], and the metazido derivative, at a somewhat higher resolution, by Hodgson and co-workers [27]. Apart from deoxyhemerythrin, all forms possessed a  $\mu$ -oxo bridged binuclear iron site with similar first shell

EXAFS [26,27]. For deoxyhemerythrin, the lack of an Fe-Fe interaction in the range for a  $\mu$ -oxo bridged site indicated the lack of a  $\mu$ -oxo bridge in this form [26]. Both met- and azidomet-hemerythrin have been studied by X-ray crystallography at 2.0 Å resolution [28]. The active site of the protein is a binuclear iron site with two carboxylate bridges and one  $\mu$ -oxo bridge, the other ligands to iron are all histidines in methemerythrin; one iron possessing two and the other three. In azidomethemerythrin the azide is coordinated to the iron that is five coordinate in methemerythrin. The crystallographically determined Fe- $\mu$ -oxo distances are extremely asymmetric, especially for methemerythrin; 1.92 Å from the six coordinate iron, and 1.68 Å from the five coordinate iron. The crystallographic results for azidomethemerythrin are in general agreement with those from EXAFS apart from a somewhat different Fe-Fe distance (3.25 Å versus 3.38 Å for EXAFS).

Ribonucleotide reductase (EC 1.17.4.1) catalyzes the reduction, by thioredoxin or glutaredoxin, of ribonucleotides to the corresponding deoxyribonucleotides, and so provides a key control point for the regulation of DNA synthesis. Its active site contains a tyrosine radical stabilized by a  $\mu$ -oxo linked binuclear iron site, where both the irons are ferric [13]. The optical spectrum of the radical-containing ribonucleotide reductase has a prominent feature at 410 nm, and broad features at 530, 600 and 680 nm; all of these are attributable to the tyrosyl radical [29]. The iron atoms are ESR-silent, but the tyrosine radical gives rise to a distinct asymmetric doublet centered at  $g$  2.0047 [13]. The optical spectrum of the hydroxylase (Fig. 1) shows some similarity to that of ribonucleotide reductase, but no ESR signals similar to those of the tyrosyl radical in the latter were detected. Some samples of hydroxylase displayed isotropic signals near  $g$  2.0025, suggestive of organic free-radicals, but they were not present in all samples, and may well be contaminants. Furthermore, the optical spectrum of the hydroxylase was essentially unaffected by excess reductant in the form of sodium dithionite; although not explicitly stated in the study of the tyrosine radical of ribonucleotide reductase by Sjöberg et al. [30], its properties suggest that it would be readily reduced to the tyrosine ground state by such a reductant, with a

bleaching of the 410 nm band. The EXAFS spectrum of the iron site of ribonucleotide reductase [31] is very similar to that of azidomethemerythrin [26], although there are indications that at least one of the terminal nitrogenous ligands of each iron in the latter are replaced by oxyanions such as hydroxide, phenolate or carboxylate [31].

Purple acid phosphatases are widespread in mammalian, plant and bacterial sources. As their name suggests, they are intensely purple proteins with phosphatase activity, but their physiological functions have not been well defined [14]. Many of these purple acid phosphatases contain a binuclear iron active site, although Fe-Zn and Mn centers have also been described [32]. Perhaps the best characterized binuclear iron enzyme is from bovine spleen. As isolated, in the purple form (absorption maxima at 280 and 550 nm [33]), it is ESR-silent, but treatment with mild reductant converts the enzyme to the pink (absorption maxima at 280 and 500 nm [33]), active form with an ESR signal with  $g_{av}$  near 1.77 [34]. No additional or alternative signals are seen under conditions where the  $g_{av}$  1.74 signal of the hydroxylase is visible. The purple acid phosphatases show no absorption maxima near 408 nm in any known form [33]. The EXAFS spectra of the bovine spleen enzyme [35] indicate an Fe-Fe distance of 3.00 Å, consistent with a bridged binuclear iron center, but Fe-O(tyrosine) linkages at 1.8–1.9 Å precluded direct observation of the expected bridging oxo group.

Uteroferrin is isolated from uterine flushings of animals with epitheliochorial placentation, such as the sow and mare. It can account for up to a third of the protein in the uterine fluid, turning it distinctly purple [14]. Its abundance, and its iron-content, suggested a role in iron-transfer from mother to fetus; hence the euphonious relation to transferrin [14]. The spectroscopic properties of uteroferrin suggest that the iron cluster is very similar to that of the purple acid phosphatases. The purple form is ESR-silent, but mild reduction to the pink form reveals an ESR signal with  $g_{av}$  1.76 [14].

While the hydroxylase shares some common features with hemerythrin, ribonucleotide reductase, purple acid phosphatases and uteroferrin, it also has several unique features. The absorption

spectrum is different from any of them, although as discussed above, it shares a band near 410 nm with ribonucleotide reductase. In the latter, this is due to a tyrosyl radical with distinctive ESR properties. As discussed above, such a species would be predicted to be reducible, and hence bleached, by dithionite. Neither the ESR spectrum nor the bleaching is seen in the hydroxylase. An alternative identification for the 408 nm peak in the hydroxylase is that it is a metallo-porphyrin. Since it is unchanged by oxidant or reductant, the metal might be a redox-inactive metal such as zinc (0.5 Zn per enzyme, see Refs. 9 and 15), and indeed preliminary resonance raman spectra suggest the presence of zinc-porphyrin in some samples of the hydroxylase (Czernuszewicz, R., Macor, K.A., Patel, R.N. and Spiro, T.G., unpublished observations). If this identification is correct, the low zinc content of the enzyme raises doubts as to its physiological significance, for Zn porphyrins are common artifacts in microbial extracts [36].

The ESR spectra of the hydroxylase share several similarities with those of semimethemerythrin and the pink forms of purple acid phosphatase and uteroferrin, although none of the latter have been shown to have signals as difficult to saturate as the  $g_{av}$  1.73 signal of the hydroxylase. All the available data on the signals from the hydroxylase seem entirely consistent with the presence of a spin-coupled mixed valence  $\mu$ -oxo bridged binuclear iron site. The  $g_{av}$  1.73 species clearly possesses some potent method of relaxation, most probably associated with low lying excited states. The maximal spin-count per enzyme for the hydroxylase has been 0.5–0.6, but only in the presence of the redox mediator *N*-methylphenazonium methosulfate, (but note that this is an underestimate due to the presence of the broad signal at  $g$  2.05). The enzyme as prepared shows only 0.05–0.07 spins per molecule, and all of these in the form of the  $g_{av}$  1.74 signal. It is this form, in the absence of the mediator, that has been characterized by X-ray spectroscopy.

The presence of an iron–iron interaction at 3.05 Å is consistent with a binuclear iron site similar to those discussed above. However, because of the limit of resolution for similar ligand types afforded by the  $k$ -range of our EXAFS data (about 0.27 Å, cf. Ref. 37) no direct conclusions as

presence of absence of  $\mu$ -oxo or  $\mu$ -hydroxo ligands can be drawn. Nevertheless, such a short Fe-Fe distance is difficult to reconcile with any structure other than those with  $\mu$ -oxo or  $\mu$ -hydroxo bridges. The edge data are consistent with octahedrally coordinated ferric iron, and the EXAFS is not inconsistent with this, with a coordination between 4 and 6. The amplitude of the Fe-Fe interaction seems large for a binuclear structure and we cannot exclude the possibility of some more complex type of iron cluster. However, it should be noted that the long distance interaction may have small contributions from outer shell carbons from histidine or tyrosine ligands to iron which would artefactually enhance the measured Fe-Fe amplitude.

Overall our conclusion is that the iron site of the hydroxylase is most likely a binuclear cluster similar to the  $\mu$ -oxo- or  $\mu$ -hydroxo-bridged sites characterized in other systems. The resting state appears to contain largely ferric iron, while the reduced forms give ESR signals consistent with a ferric-ferrous spin coupled system.

### Acknowledgements

We are grateful to Drs. S. Gorun and E.I. Stiefel for helpful comments and encouragement during this work, and to R. Czernuszewicz, K.A. Macor and T.G. Spiro for permission to quote their unpublished work. We are also grateful to O.T.G. Jones for helpful discussions on Zn-porphyrins in natural systems, and are indebted to the staff of SSRL for their assistance with the X-ray work. SSRL is supported by the Department of Energy, Office of Basic Energy Sciences, and the National Institutes of Health, Biotechnology Resource Program.

### References

- 1 Anthony, C. (1982) *The Biochemistry of Methylotrophs*, Academic Press, New York.
- 2 Haber, C.L., Allen, L.N., Zhao, S. and Hanson, R.S. (1983) *Science* 221, 1147–1153.
- 3 Stanley, S.H., Prior, S.D., Leak, D.J. and Dalton, H. (1983) *Biotech. Lett.* 5, 487–492.
- 4 Cornish, A., MacDonald, J., Burrows, K.J., King, T.S., Scott, D. and Higgins, I.J. (1985) *Biotech. Lett.* 7, 319–324.
- 5 Colby, J. and Dalton, H. (1978) *Biochem. J.* 171, 461–468.
- 6 Patel, R.N., Hou, C.T., Laskin, A.J. and Felix, A. (1982) *Appl. Env. Microbiol.* 44, 1130–1137.
- 7 Tonge, G.M., Harrison, D.E.F. and Higgins, I.J. (1977) *Biochem. J.* 161, 333–344.
- 8 Woodland, M.P., Patil, D.S., Cammack, R. and Dalton, H. (1986) *Biochim. Biophys. Acta* 873, 237–242.
- 9 Patel, R.N. (1984) in *Proc. 4th Int. Symp. on Microbial Growth on Cl Compounds* (Crawford, R.L. and Hanson, R.S., eds.), pp. 83–90, Am. Soc. Microbiol. Washington, D.C.
- 10 Lund, J., Woodland, M.P. and Dalton, H. (1985) *J. Biol. Chem.* 260, 15795–15801.
- 11 Prince, R.C. and Patel, R.N. (1986) *FEBS Lett.* 203, 127–130.
- 12 Wilkins, R.G. and Harrington, P.C. (1983) *Adv. Inorg. Biochem.* 5, 51–85.
- 13 Reichard, P. and Ehrenberg, A. (1983) *Science* 221, 514–519.
- 14 Antanaitis, B.C. and Aisen, P. (1983) *Adv. Inorg. Biochem.* 5, 111–136.
- 15 Patel, R.N. and Savas, J.C. (1987) *J. Bact.* 169, 2313–2317.
- 16 Aasa, R. and Vanngard, T. (1975) *J. Mag. Res.* 19, 308–315.
- 17 Cramer, S.P. and Scott, R.A. (1981) *Rev. Sci. Instrum.* 52, 395–399.
- 18 Lytle, F.W., Greeger, R.B., Sandstrom, D.R., Marques E.C., Wong, J., Spiro, C.L., Huffman, G.P. and Higgins, F.E. (1984) *Nucl. Instr. Methods A* 226, 542–548.
- 19 Teo, B.K. and Lee, P.A. (1979) *J. Am. Chem. Soc.* 101, 2815–2823.
- 20 Woodland, M.P. and Dalton, H. (1984) *J. Biol. Chem.* 259, 53–59.
- 21 Prince, R.C., Linkletter, S.J.G. and Dutton, P.L. (1981) *Biochim. Biophys. Acta* 635, 132–148.
- 22 Shulman, R.G., Yafet, Y., Eisenberger, P. and Blumberg, W.E. (1976) *Proc. Natl. Acad. Sci. USA* 73, 1384–1388.
- 23 Cramer, S.P. (1977) Ph.D. Thesis, Stanford University, Stanford.
- 24 Garbett, K., Darnall, D.W., Klotz, I.M. and Williams, R.J.P. (1969) *Arch. Biochem. Biophys.* 135, 419–434.
- 25 Muhoberac, B.B., Wharton, D.C., Babcock, L.M., Harrington, P.C. and Wilkins, R.G. (1980) *Biochim. Biophys. Acta* 626, 337–345.
- 26 Elam, W.T., Stern, E.A., McCallum, J.D. and Sanders-Loehr, J. (1982) *J. Am. Chem. Soc.* 104, 6369–6373.
- 27 Hendrickson, W.A., Co, M.S., Smith, J.L., Hodgson, K.O. and Klippenstein, G.L. (1982) *Proc. Natl. Acad. Sci. USA* 79, 6255–6259.
- 28 Stenkamp, R.E., Sieker, L.C. and Jensen, L.H. (1984) *J. Am. Chem. Soc.* 106, 618–622.
- 29 Petersson, L., Graslund, A., Ehrenberg, A., Sjoberg, B. and Reichard, P. (1980) *J. Biol. Chem.* 255, 6706–6712.
- 30 Sjoberg, B., Reichard, P., Graslund, A. and Ehrenberg, A. (1977) *J. Biol. Chem.* 252, 536–541.
- 31 Scarrow, R.C., Maroney, M.J., Palmer, S.M., Que, L., Sallow, S.P. and Stubbe, J. (1986) *J. Am. Chem. Soc.* 108, 6832–6834.
- 32 Beck, J.L., McConachie, L.A., Summors, A.C., Arnold, W.N., De Jersey, J. and Zerner, B. (1986) *Biochim. Biophys. Acta* 869, 61–68.

- 33 Davis, J.C., Lin, S.S. and Averill, B.A. (1981) *Biochemistry* 20, 4062–4067.
- 34 Davis, J.C. and Averill, B.A. (1982) *Proc. Natl. Acad. Sci. USA* 79, 4623–4627.
- 35 Kauzlarich, S.M., Teo, B.K., Zirino, T., Burman, S., Davis, J.C. and Averill, B.A. (1986) *Inorg. Chem.* 25, 2781–2785.
- 36 Pretlow, T.P. and Sherman, F. (1967) *Biochim. Biophys. Acta* 148, 629–644.
- 37 Shulman, R.G., Eisenburger, P., Blumberg, W.E. and Stombaugh, N.A. (1975) *Proc. Natl. Acad. Sci. USA* 72, 4003–4007.
- 38 Beinert, H. and Orme-Johnson, W.H. (1967) in *Magnetic Resonance in Biological Systems* (Ehrenberg, A., Malmstrom, B.G. and Vanngard, T., eds.), p. 221, Pergamon Press, Oxford, U.K.